JOURNAL OF THE AMERICAN COLLEGE OF CARDIOLOGY
PUBLISHED BY ELSEVIER ON BEHALF OF THE AMERICAN
COLLEGE OF CARDIOLOGY FOUNDATION

VOL. 75, NO. 1, 2020

ORIGINAL INVESTIGATIONS

Persistent Proarrhythmic Neural Remodeling Despite Recovery From Premature Ventricular Contraction-Induced Cardiomyopathy

Alex Y. Tan, MD,[a,b] Khalid Elharrif, MD,[a,b] Ricardo Cardona-Guarache, MD, MPH,[a,b] Pranav Mankad, MD,[a,b] Owen Ayers, BA,[b] Martha Joslyn, MS,[b] Anindita Das, PhD,[a] Karoly Kaszala, MD, PhD,[a,b] Shien-Fong Lin, PhD,[c] Kenneth A. Ellenbogen, MD,[a,b] Anthony J. Minisi, MD,[a,b] Jose F. Huizar, MD[a,b]

ABSTRACT

BACKGROUND The presence and significance of neural remodeling in premature ventricular contraction-induced cardiomyopathy (PVC-CM) remain unknown.

OBJECTIVES This study aimed to characterize cardiac sympathovagal balance and proarrhythmia in a canine model of PVC-CM.

METHODS In 12 canines, the investigators implanted epicardial pacemakers and radiotelemetry units to record cardiac rhythm and nerve activity (NA) from the left stellate ganglion (SNA), left cardiac vagus (VNA), and arterial blood pressure. Bigeminal PVCs (200 ms coupling) were applied for 12 weeks to induce PVC-CM in 7 animals then disabled for 4 weeks to allow complete recovery of left ventricular ejection fraction (LVEF), versus 5 sham controls.

RESULTS After 12 weeks of PVCs, LVEF ($p = 0.006$) and dP/dT ($p = 0.007$) decreased. Resting SNA ($p = 0.002$) and VNA ($p = 0.04$), exercise SNA ($p = 0.01$), SNA response to evoked PVCs ($p = 0.005$), heart rate (HR) at rest ($p = 0.003$), and exercise ($p < 0.04$) increased, whereas HR variability (HRV) decreased ($p = 0.009$). There was increased spontaneous atrial ($p = 0.02$) and ventricular arrhythmias ($p = 0.03$) in PVC-CM. Increased SNA preceded both atrial ($p = 0.0003$) and ventricular ($p = 0.009$) arrhythmia onset. Clonidine suppressed SNA and abolished all arrhythmias. After disabling PVC for 4 weeks, LVEF ($p = 0.01$), dP/dT ($p = 0.047$), and resting VNA ($p = 0.03$) recovered to baseline levels. However, SNA, resting HR, HRV, and atrial ($p = 0.03$) and ventricular ($p = 0.03$) proarrhythmia persisted. There was sympathetic hyperinnervation in stellate ganglia ($p = 0.02$) but not ventricles ($p = 0.2$) of PVC-CM and recovered animals versus sham controls.

CONCLUSIONS Neural remodeling in PVC-CM is characterized by extracardiac sympathetic hyperinnervation and sympathetic neural hyperactivity that persists despite normalization of LVEF. The altered cardiac sympathovagal balance is an important trigger and substrate for atrial and ventricular proarrhythmia. (J Am Coll Cardiol 2020;75:1–13) Published by Elsevier on behalf of the American College of Cardiology Foundation.

Listen to this manuscript's audio summary by Editor-in-Chief Dr. Valentin Fuster on JACC.org.

From the [a]Pauley Heart Center, Virginia Commonwealth University, Richmond, Virginia; [b]Electrophysiology Section, Division of Cardiology, Hunter Holmes McGuire VA Medical Center, Richmond, Virginia; and the [c]Krannert Institute of Cardiology, Indiana University School of Medicine, Indianapolis, Indiana. Dr. Tan receives research grants from American Heart Association (AHA SDG 16SDG31280012). Dr. Huizar has received research grants from National Institutes of Health (1R56HL133182-01); and has received research support from St. Jude Medical. Dr. Kaszala has received research support from Boston Scientific Corp and St. Jude Medical. Dr. Ellenbogen has received research support from Boston Scientific, Biosense Webster, Medtronic, St. Jude Medical; is a consultant for Boston Scientific, St. Jude Medical, Atricure, and Medtronic; and has received honoraria from Medtronic, Boston Scientific, Biotronik, Biosense Webster, and Atricure. All other authors have reported that they have no relationships relative to the contents of this paper to disclose.

Manuscript received July 11, 2019; revised manuscript received September 30, 2019, accepted October 21, 2019.

ISSN 0735-1097/$36.00 https://doi.org/10.1016/j.jacc.2019.10.046

ABBREVIATIONS AND ACRONYMS

CANS = cardiac autonomic nervous system

LVEDV = left-ventricular end-diastolic volume

LVEF = left ventricular ejection fraction

NA = nerve activity

PAT = paroxysmal atrial tachyarrhythmia

PVC = premature ventricular complex

PVC-CM = PVC-induced cardiomyopathy

VNA = vagal nerve activity

SG = stellate ganglia

SNA = sympathetic NA

SR = sinus rhythm

Frequent premature ventricular contractions (PVCs) can cause nonischemic cardiomyopathy (CM) (1), resulting in systolic heart failure (2). PVC-induced CM (PVC-CM) is a unique form of CM characterized by LV systolic dysfunction that is reversible upon successful PVC suppression (1-3). However, lethal ventricular arrhythmias and sudden cardiac death have been reported in patients with PVC-CM (4). Autonomic imbalance—specifically, sympathetic upregulation—has been postulated to contribute both to the pathogenesis of PVC-CM and its proarrhythmic consequences (**Central Illustration, panel A**). The hypothesis is based upon studies demonstrating PVCs as a powerful acute stressor of the cardiac autonomic nervous system (CANS) (5,6). However, longer-term CANS function of the CANS when exposed to chronic PVCs, and its relationship with arrhythmogenesis remain unknown. We recently reported that application of chronic bigeminal PVCs in a canine model for 12 weeks (7,8) resulted in PVC-CM that was fully reversible 4 weeks after disabling PVCs. The goal of the current study was to perform chronic ambulatory recordings of cardiac sympathetic nerve activity (SNA) and vagal nerve activity (VNA) (9) in our canine model of PVC-CM to characterize cardiac sympathovagal balance and arrhythmogenesis during the development and subsequent resolution of PVC-CM. We hypothesize that neural remodeling occurs in PVC-CM, resulting in elevation in cardiac sympathetic tone, which, in turn, is proarrhythmic (**Central Illustration, panels A to C**).

SEE PAGE 14

METHODS

The protocol was approved by the Institutional Animal Care and Use Committee and conformed to the National Institute of Health's Guide for the Care and Use of Laboratory Animals. We studied 12 mongrel canines (20 kg to 30 kg), consisting of 7 experimental animals and 5 sham controls. **Figure 1A** diagrams the experimental protocol. The experimental group underwent chronic bigeminal PVC exposure for 12 weeks then disabled for 4 weeks to allow LV function to recover (7). Sham controls underwent identical first surgery and chronic instrumentation as the experimental group, followed by serial assessments of NA at 2, 4, and 8 weeks during sinus rhythm (SR) without PVCs, before final surgery.

FIRST SURGERY. We implanted a bipolar epicardial pacing electrode (Boston Scientific, Minneapolis, Minnesota) in the right-ventricular (RV) apex and connected it to a pacemaker (St. Jude Medical, St. Paul, Minnesota) as described previously (7). We also implanted a radiotelemetry device (Data Sciences International, Minneapolis, Minnesota) to record NA (**Figure 1B**) from the left stellate ganglion (SNA), cardiac branch of the left thoracic vagus nerve (VNA), electrocardiogram (ECG), and central arterial blood pressure (9) (see Online Methods for details).

Autonomic nerve data acquisition and analyses. Following 2 weeks of post-operative recovery (**Figure 1A**), NA, blood pressure (BP), and ECG were acquired for 72 h in SR (baseline). Bigeminal PVCs (coupling 200 ms, **Figure 1C**) was then enabled for 12 weeks in the experimental group, using a novel premature pacing algorithm (7). PVCs were disabled after the development of PVC-CM, confirmed by transthoracic echocardiography (TTE) (7). Telemetry recordings were repeated for 72 h in SR (PVC-CM). PVCs remained disabled for a further 4 weeks to allow full recovery of LV systolic function (7). Following this, 72-h recordings were repeated in SR (recovery). The methods for quantifying NA have been reported previously (9) and are detailed in the Online Methods.

Pharmacologic validation of neural recordings. We performed pharmacologic challenges with intravenous clonidine (10 μg/kg) and phenylephrine (0.1 mg) to further verify that our recordings represented efferent sympathetic and vagal nerve traffic, respectively (Online Methods).

Transthoracic echocardiography and exercise tolerance test. Echocardiography (Vivid-7, GE-Echopac Version 7.3.0, GE Medical Systems, Boston, Massachusetts) was performed in SR as described previously and expanded in the Online Methods (7,8).

Spontaneous arrhythmias. We manually analyzed 24-h periods of SR during baseline, PVC-CM, and recovery to determine the incidence of spontaneous atrial and ventricular arrhythmias (Online Methods).

Acute PVC challenge. We determined the autonomic response to acute PVC challenge during baseline, PVC-CM, and recovery. Animals were exposed to 1 min of quadrigeminal PVCs (200 ms coupling). NA and systolic BP were quantified in 30-s segments before and after onset of PVC (see expanded Online Methods).

FINAL SURGERY. A left thoracotomy was created. Animals were euthanized. Tissues were harvested and preserved in 4% formaldehyde overnight and stored in 70% alcohol until histological processing.

CENTRAL ILLUSTRATION **Neural Remodeling in Premature Ventricular Contraction-Induced Cardiomyopathy**

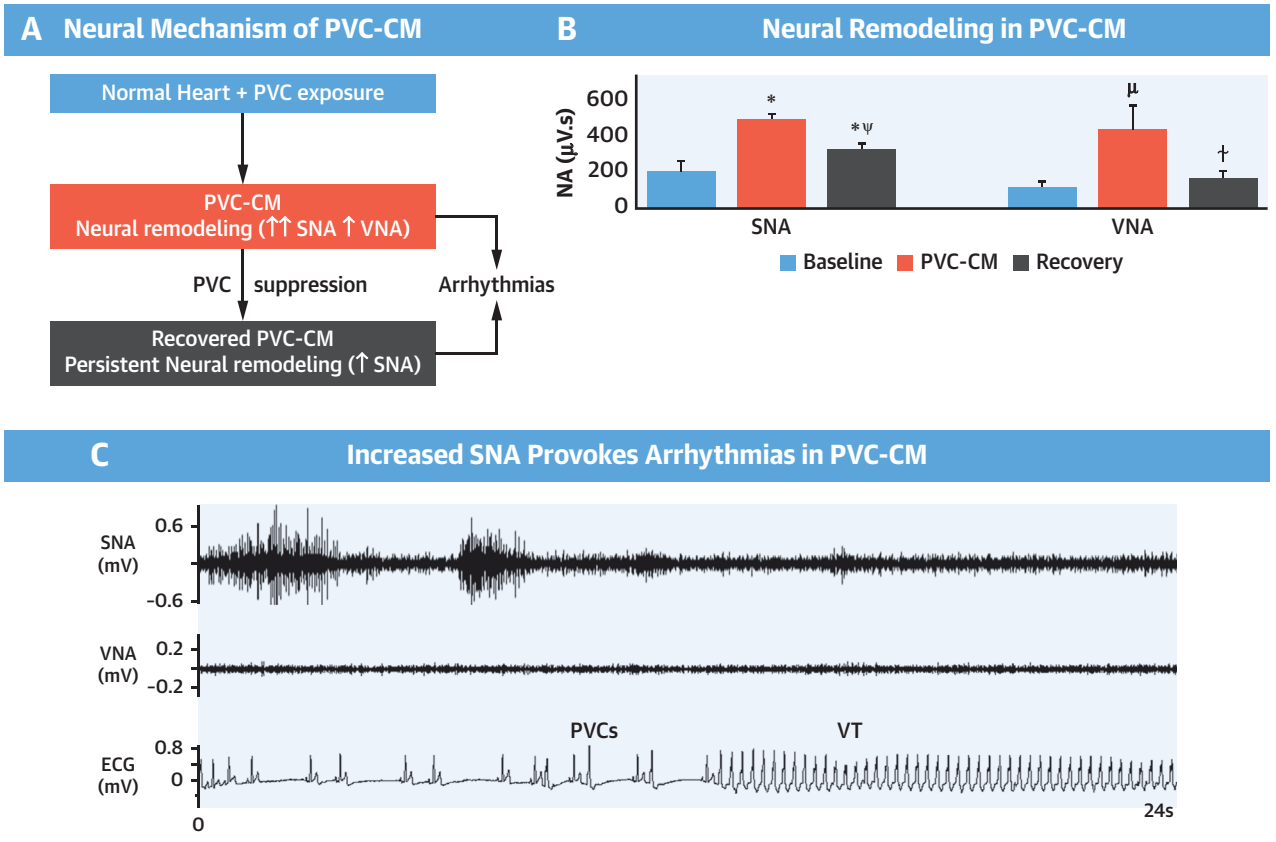

Tan, A.Y. et al. J Am Coll Cardiol. 2020;75(1):1-13.

(A) Proposed neural mechanism of premature ventricular contraction-induced cardiomyopathy (PVC-CM) and consequent proarrhythmia. Chronic frequent PVCs cause PVC-CM and neural remodeling. **(B)** Neural remodeling in PVC-CM is characterized by increased SNA and VNA. Neural remodeling (increased SNA) persists despite recovery from PVC-CM. **(C)** In neurally remodeled hearts in PVC-CM and recovered PVC-CM, increased SNA triggers ventricular arrhythmias. *p < 0.01 versus baseline; μ p < 0.05 versus baseline; + p < 0.05 versus PVC-CM; ψ p < 0.01 versus PVC-CM. ECG = electrocardiogram; PVC-CM = premature ventricular contraction-induced cardiomyopathy; SNA = sympathetic nerve activity; VNA = vagal nerve activity; VT = ventricular tachycardia

Histology. Ventricular (RV, LV free wall, and apex) and neural tissue (left and right stellate ganglia [SG], left cardiac vagus) from the 7 animals in the experimental cohort (recovered PVC-CM), 5 sham normal controls and 5 historical unrecovered PVC-CM controls were paraffin embedded, cut into 5-μm sections, mounted on glass slides, and examined under light microscopy. The unrecovered PVC-CM controls underwent a similar chronic PVC protocol as the experimental group but without a recovery phase. The sections were stained with hematoxylin and eosin and Mason's trichrome and immunostained with tyrosine hydroxylase (TH) and choline acetyltransferase (ChAT) antibodies to highlight adrenergic and cholinergic neurons respectively (10). Quantitative analyses of immunostaining (TH, ChAT) and myocardial fibrosis (Mason's trichrome) was performed using Image J software version 1.8.0 (NIH Java, Bethesda, Maryland).

Statistical analyses. Data were expressed as mean ± SEM. Repeated measures analysis of variance (ANOVA) (with Bonferroni post hoc analyses) was used to compare the means among baseline, PVC-CM, and recovery. For nonparametric comparisons, a chi-square test was used. A p value <0.05 was considered statistically significant.

RESULTS

The study period was 152 ± 3 days for the experimental group and 58 ± 2 days for the sham control group. After 12 weeks of bigeminal PVC exposure, all

FIGURE 1 Experimental Protocol

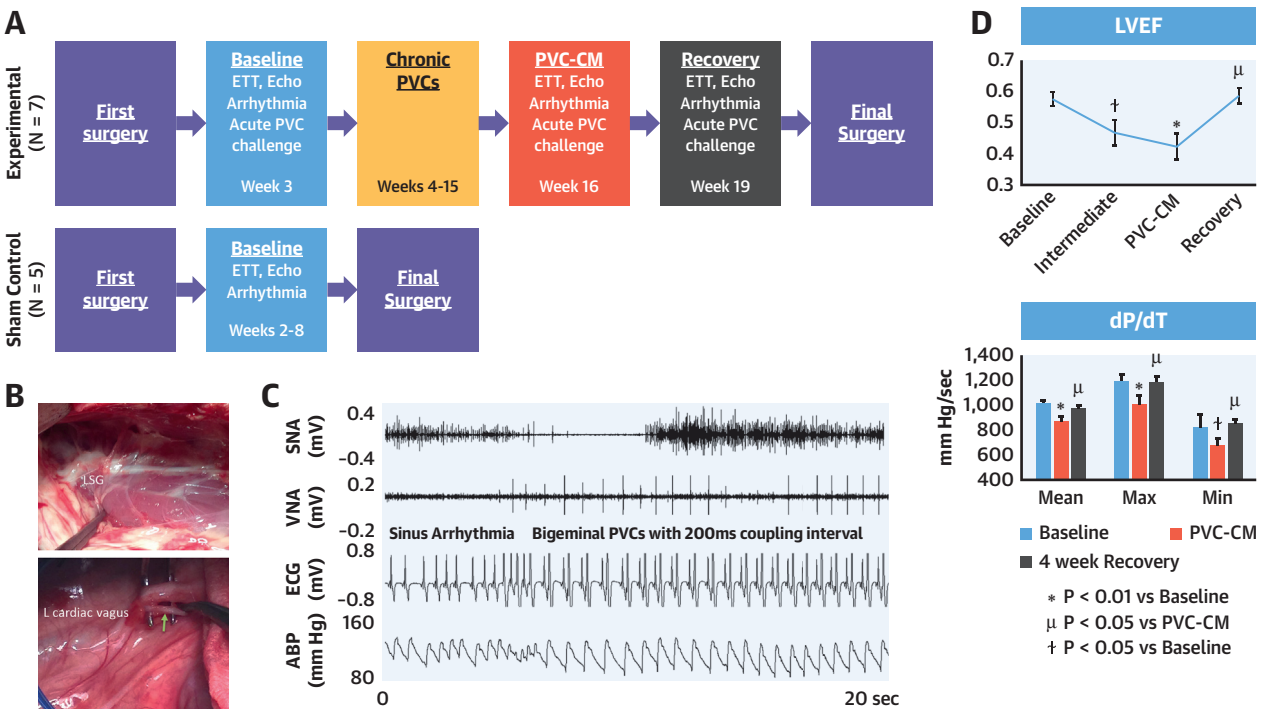

(A) Sequence of events. **(B)** Left thoracotomy showing left stellate ganglion and cardiac branch of left thoracic vagal nerve (**arrow**). **(C)** Initiation of bigeminal PVC associated with SNA increase. **(D)** Left ventricular ejection fraction (LVEF) and dP/dT during development of and recovery from PVC-induced cardiomyopathy (PVC-CM). Intermediate stage was obtained after 4 weeks of bigeminal PVC exposure. ABP = arterial blood pressure; dP/dT = rate of change of pressure with time; ETT = exercise treadmill test; SNA = sympathetic nerve activity; VNA = vagal nerve activity.

experimental animals developed PVC-CM (Figure 1D). Table 1 summarizes all results. Figure 1D illustrates the serial changes in left-ventricular ejection fraction (LVEF) ($p = 0.006$) and rate of change of pressure with time (dP/dT) ($p = 0.007$), which decreased significantly in PVC-CM compared with baseline. After disabling PVCs for 4 weeks, LVEF ($p = 0.001$ vs. PVC-CM, $p = 0.38$ vs. baseline) and dP/dT ($p = 0.046$ vs. PVC-CM, $p = 0.31$ vs. baseline) recovered to baseline values. Left-ventricular end-diastolic volume (LVEDV) (Table 1) remained increased ($p = 0.029$ vs. baseline).

PHARMACOLOGIC VALIDATION OF NEURAL RECORDINGS. Please refer to Online Materials for details.

AUTONOMIC NERVE ACTIVITY AT REST. Figure 2 demonstrates diurnal profiles of resting SNA (Figure 2A) and VNA (Figure 2B) in SR at 3 stages: baseline, PVC-CM, and recovery. Figure 2C demonstrates mean 24-h resting SNA and VNA in experimental versus sham control groups. Table 1 summarizes the NA averages as well as mean resting heart rate (HR) and heart rate variability (HRV) of the experimental group. There was a significant increase in SNA ($p = 0.002$) and VNA ($p = 0.04$) in PVC-CM compared with baseline and correlated with increased mean resting HR ($p = 0.037$) and reduced HRV ($p = 0.009$). After LVEF recovery, resting SNA decreased compared with PVC-CM ($p = 0.009$) but not with baseline levels ($p = 0.004$ vs. baseline). In contrast, resting VNA recovered fully to baseline levels ($p = 0.035$ vs. PVC-CM, $p = 0.15$ vs. baseline). However, mean resting HR ($p = 0.04$) remained elevated, and HRV ($p = 0.045$) remained decreased compared with baseline. In contrast, resting SNA and VNA in the sham control group were unchanged through weeks 2, 4, and 8 after first surgery ($p = 0.79$).

AUTONOMIC NERVE ACTIVITY DURING EXERCISE TREADMILL TEST. Figure 3A is a profile of SNA during 5 min pre-exercise, followed by a 9-min exercise treadmill test (ETT) and subsequent 10-min recovery in SR. Compared with baseline, mean exercise SNA during ETT was increased in PVC-CM ($p < 0.01$, Figure 3B). Following recovery from PVC-CM, exercise

SNA decreased compared with PVC-CM ($p = 0.014$), but it remained elevated compared with baseline ($p = 0.048$). Exercise VNA (Figure 3B) was also increased in PVC-CM ($p = 0.01$) compared with baseline. Unlike SNA, exercise VNA was restored to baseline levels ($p = 0.21$) in recovered PVC-CM. Mean ($p = 0.037$) and maximum HR ($p = 0.042$) during exercise (Figure 3B) were both higher in PVC-CM compared with baseline. After recovery, mean ($p = 0.039$ vs. PVC-CM, $p = 0.44$ vs. baseline) and maximum ($p = 0.049$ vs. PVC-CM, $p = 0.17$ vs. baseline) exercise HR recovered to baseline levels.

SPONTANEOUS ARRHYTHMIAS. Table 1 compares arrhythmia frequency between baseline, PVC-CM, and recovery. Figure 4 illustrates an example of spontaneous paroxysmal atrial tachyarrhythmia (PAT) (Figure 4A), nonsustained (<30 s) ventricular tachycardia (NSVT) (Figure 4B), and PVC (Figure 4C). Note that there was increased SNA and VNA before onset of PAT and increased SNA alone before onset of ventricular tachycardia (VT) or PVC. Figure 5A compares arrhythmia frequency at different stages. There was a significant increase in the incidence of PAT ($p = 0.02$) in PVC-CM compared with baseline. There was no difference in mean PAT cycle length (309 ± 6 ms vs. 291 ± 12 ms, $p = 0.09$), but total duration of PAT was longer in PVC-CM compared with baseline ($1,486 \pm 187$ s vs. 710 ± 204 s, $p = 0.004$). Increased atrial arrhythmia burden persisted in recovery (frequency: 77 ± 25 episodes per day vs. 34 ± 10 episodes per day vs. baseline, $p = 0.03$; duration: $1,125 \pm 198$ s vs. 710 ± 204 s vs. baseline, $p = 0.03$). No animals had spontaneous ventricular arrhythmias at baseline, whereas spontaneous PVCs (total 34 episodes) and NSVT (total 19 episodes) were observed in 3 of 7 animals during CM (PVCs: 20 episodes, NSVT: 10 episodes, $p = 0.03$ vs. baseline) and in 3 of 7 animals in recovery (PVCs: 14 episodes, NSVT: 9 episodes, $p = 0.03$ vs. baseline). No animals developed sustained (>30 s) VT or sudden cardiac death.

TABLE 1 Results Summary

	Baseline	PVC-CM	Recovery
LVEF, %	58 ± 2	42 ± 4	59 ± 2
p value vs. baseline		0.006	0.38
p value recovery vs. PVC-CM			0.001
LVEDV, ml	47 ± 2.8	61.4 ± 4.6	56.7 ± 2.3
p value vs. baseline		0.016	0.029
p value recovery vs. PVC-CM			0.17
dP/dT, mm Hg/s	1,015 ± 24	870 ± 40	977 ± 21
p value vs. baseline		0.007	0.31
p value recovery vs. PVC-CM			0.046
Mean resting HR, beats/min	69 ± 2	92 ± 6	80 ± 5
p value vs. baseline		0.004	0.04
p value recovery vs. PVC-CM			0.22
Mean exercise HR, beats/min	142 ± 4	156 ± 2	143 ± 9
p value vs. baseline		0.037	0.44
p value recovery vs. PVC-CM			0.039
HR variability 24-h SDRR (s)	0.5 ± 0.04	0.38 ± 0.02	0.41 ± 0.06
p value vs. baseline		0.009	0.045
p value recovery vs. PVC-CM			0.18
Mean resting SNA, μV.s	199 ± 5	480 ± 28	320 ± 31
p value vs. baseline		0.002	0.004
p value recovery vs. PVC-CM			0.009
Mean exercise SNA, μV.s	698 ± 38	1,266 ± 155	859 ± 98
p value vs. baseline		0.014	0.048
p value recovery vs. PVC-CM			0.07
Mean resting VNA, μV.s	115 ± 30	423 ± 129	165 ± 33
p value vs. baseline		0.04	0.15
p value recovery vs. PVC-CM			0.03
Mean exercise VNA, μV.s	566 ± 44	1,024 ± 58	668 ± 36
p value vs. baseline		0.025	0.21
p value recovery vs. PVC-CM			0.05
Atrial tachyarrhythmia, episodes/day	34 ± 10	87 ± 22	77 ± 25
p value vs. baseline		0.02	0.03
p value recovery vs. PVC-CM			0.14
Animals with ventricular arrhythmia	0	3/7 (20 episodes)	3/7 (19 episodes)
p value vs. baseline		0.03	0.03
p value recovery vs. PVC-CM			0.99

Values are mean ± SD; 3/7 refers to 3 out of 7 animals; number in parentheses refers to the total number of episodes of ventricular arrhythmia in that group. dP/dT = rate of change of pressure with time; HR = heart rate; LVEDV = left-ventricular end diastolic volume; LVEF = left-ventricular ejection fraction; SNA = sympathetic nerve activity; VNA = vagal nerve activity.

Figure 5B summarizes NA quantitation at onset of arrhythmia. There was a surge in SNA ($p = 0.0003$) and VNA ($p = 0.004$) within 10 s of PAT onset (vs. 60 s before onset). SNA increase preceded VNA increase by 20 s (-30 s vs. -10 s). SNA peak in the 10 s before onset of PAT was higher than mean daily 10-s SNA levels during CM (214 ± 44 vs. 160 ± 9 μV.s, $p = 0.02$). VNA peak before onset of PAT (79 ± 15 μV.s) was higher than mean daily 10-s VNA levels at baseline (38 ± 10 μV.s, $p = 0.004$) but not CM (141 ± 43 μV.s, $p = 0.1$). In contrast to atrial arrhythmias, only SNA was significantly increased before onset of ventricular arrhythmia (Figure 5C). This increase occurred within 3 s of arrhythmia onset ($p = 0.046$ vs. 5 s before onset) and peaked within 1 s of arrhythmia onset ($p = 0.009$ vs. 5 s before onset). The peak SNA levels before onset of ventricular arrhythmia was significantly higher than the mean daily 1-s SNA levels (24 ± 3 μV.s vs. 7 ± 2 μV.s, $p = 0.03$). To determine whether NA was a trigger for arrhythmias, we administered intravenous (IV) clonidine (10 μg/kg), a central imidazoline receptor antagonist known to suppress central sympathetic output, and monitored the frequency of arrhythmias within the first 4 h of administration. This time period is equivalent to 12 distribution half-lives ($T_{1/2} = 20$ min) of IV clonidine, incorporates the

FIGURE 2 Changes in Resting SNA and VNA With Development of and Recovery From PVC-CM

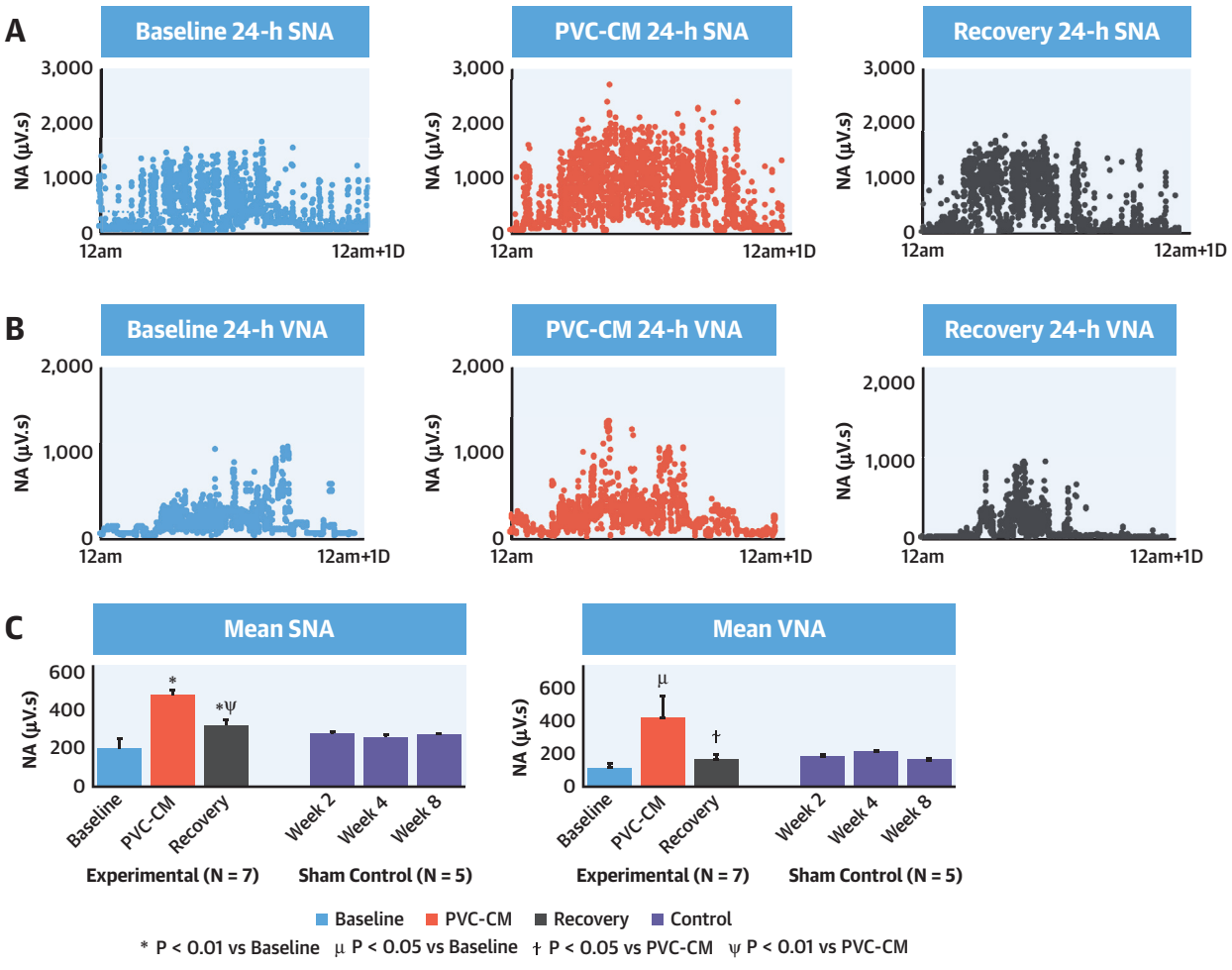

Diurnal profiles of resting SNA **(A)** and VNA **(B)** during 24 h of SR at baseline, PVC-CM and after recovery from PVC-CM. Every point represents 30-s integrated NA. **(C)** Mean 24-h resting SNA and VNA in experimental versus sham control groups. Abbreviations as in Figure 1.

peak clonidine effect (1 h) and well within its 12-h elimination half-life. IV clonidine significantly diminished both SNA ($p < 0.0001$) (Online Figure 1A) and abolished both atrial ($p = 0.0003$) and ventricular arrhythmias ($p = 0.01$) at all stages, including PVC-CM and recovery.

AUTONOMIC RESPONSE TO ACUTE PVC CHALLENGE. Figure 6 illustrates the autonomic response to a 1-min acute PVC challenge performed during SR at baseline, PVC-CM, and recovery. Acute SNA discharge (Figure 6A) occurred within seconds after PVC onset. Figure 6B is a graphical representation of integrated SNA and VNA and mean systolic BP during each 5-s period, before and after onset of PVC. Figure 6C compares 5-s integrated SNA and VNA and mean systolic arterial BP before and after onset of PVC. There was increased SNA discharge in the 30-s period after onset of PVC. The acute SNA response to PVCs was greater and more sustained in PVC-CM compared with baseline. The VNA response was not significantly different after onset of PVC. PVCs induced a significant increase in systolic BP in PVC-CM and recovery but not at baseline.

HISTOLOGY. Figure 7 illustrates TH immunostaining in the right SG (RSG0 and left SG [LSG]) (Figure 7A-C) in sham normal controls, PVC-CM, and recovered PVC-CM groups. There was a significant increase in TH immunoreactivity in both LSG ($p = 0.02$) and RSG ($p = 0.008$) of PVC-CM and recovered PVC-CM animals compared with sham normal controls (Figure 7D). There was no difference in TH

FIGURE 3 SNA Response During Exercise

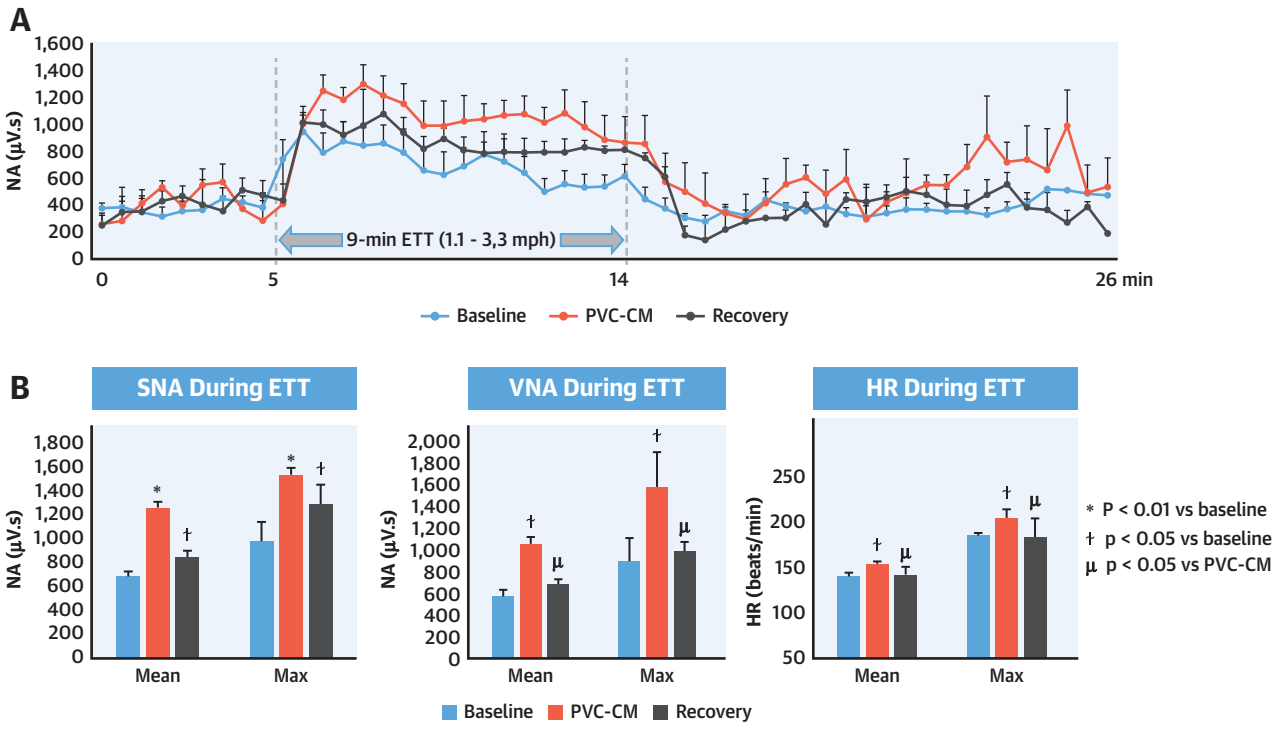

(A) SNA profile during exercise treadmill test (ETT) (up to 3.3 mph). **(B)** Mean and maximal SNA, VNA, and heart rate (HR) during ETT. Abbreviations as in Figure 1.

immunoreactivity in the SG between PVC-CM versus recovered PVC-CM ($p = 0.7$). In the ventricles (data representing mean of RV and LV regions), there was no significant difference in TH immunoreactivity (sham controls: 14 ± 1.8 vs. PVC-CM: 17.7 ± 2.7 vs. recovered PVC-CM: 13.9 ± 2 $\mu m^2/cm^2$, $p = 0.2$) or interstitial fibrosis (Figure 7E) (sham controls: 24.1 ± 7.3 vs. PVC-CM: 32.4 ± 6.3 vs. recovered PVC-CM: 35.7 ± 8.5 $\mu m^2/cm^2$, $p = 0.1$) among the 3 groups (control, PVC-CM, recovered PVC-CM).There was no difference in ChAT immunoreactivity in the left cardiac vagus nerve (Figure 7F) (control: 45.5 ± 4.2 $\mu m^2/cm^2$, PVC-CM: 49.9 ± 6.3 $\mu m^2/cm^2$, recovered PVC-CM: 51.5 ± 6.4 $\mu m^2/cm^2$, $p = 0.8$). ChAT was nonimmunoreactive in the ventricular myocardium.

DISCUSSION

We report significant and dynamic alterations of cardiac autonomic balance in the development and subsequent resolution of PVC-CM (Central Illustration).

1. SNA and VNA were both elevated in PVC-CM compared with baseline. However, increased resting and exercise HR and reduced HRV reflect net sympathetic dominance in PVC-CM.
2. Evoked RV apical PVCs (quadrigeminy, short coupled) triggered an acute increase in SNA but not VNA. In PVC-CM, the SNA response to PVCs was greater in magnitude and duration compared with baseline.
3. There was an increased incidence of spontaneous atrial and ventricular arrhythmias in PVC-CM compared with baseline. Increased SNA and VNA immediately preceded the onset of atrial arrhythmias, whereas increased SNA immediately preceded onset of ventricular arrhythmias. Clonidine suppressed SNA and all arrhythmias in the setting of PVC-CM.
4. Upon complete LVEF recovery 4 weeks after disabling PVCs, VNA recovered to baseline levels, but SNA remained elevated at rest, exercise, and in response to evoked PVCs, causing persistent sympathetic imbalance, elevated resting HR, suppressed HRV, and lack of recovery of proarrhythmia.
5. Histology demonstrated sympathetic hyperinnervation limited to SG-sparing ventricular myocardium in PVC-CM. SG hyperinnervation persisted in recovered PVC-CM.

FIGURE 4 Neural Triggers of Atrial and Ventricular Arrhythmias in PVC-CM

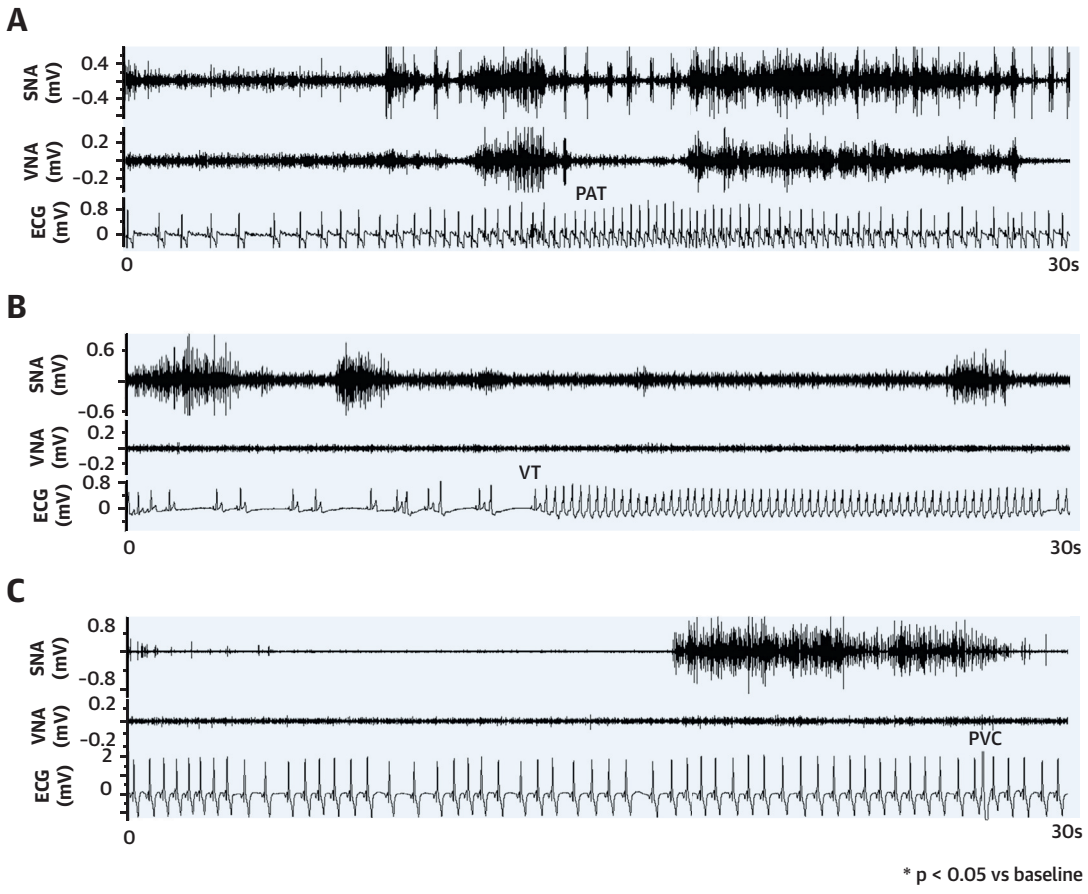

(A) Paroxysmal atrial tachyarrhythmia (PAT). **(B)** Nonsustained ventricular tachycardia (NSVT). **(C)** Premature ventricular contractions (PVCs). ECG = electrocardiogram; PVC-CM = premature ventricular contraction-induced cardiomyopathy.

Taken together, these data provide evidence of neural remodeling of the SG in PVC-CM. This remodeling persists beyond the complete recovery of LV systolic function and maintains a state of heightened cardiac sympathetic tone and proarrhythmia. These findings may have implications for patients with PVC-CM, despite successful PVC suppression strategy.

NEURAL REMODELING IN PVC-CM. After the development of PVC-CM, there were significant changes to SNA, VNA, and HR (Figures 2 and 3) that reflect net sympathetic dominance. To the best of our knowledge, this is the first demonstration of chronic sympathetic upregulation in PVC-CM. The fact that SNA upregulation persisted despite LVEF and dP/dT recovery indicates that neural remodeling has occurred in PVC-CM. On the other hand, VNA was also upregulated in PVC-CM but recovered to baseline levels after CM resolution. VNA recovery tilted autonomic balance in favor of sympathetic dominance in recovered PVC-CM. In contrast to the experimental group, the lack of change of NA in the sham control group over 8 weeks indicate that the changes of NA in the experimental group were caused by development of PVC-CM not post-surgical changes. It is important to note that NA quantitation during rest and exercise were obtained in SR rather than during PVCs to evaluate NA-HR coupling not otherwise possible with frequent PVCs. Therefore, chronic sympathetic upregulation in PVC-CM is not due to the acute effects of PVCs. Rather, they reflect a remodeled CANS reset to chronically higher SNA output by chronic PVC exposure but are independent of PVCs themselves. On the other hand, the acute effects of PVCs on NA were evaluated separately (Figure 6) and discussed further here. One advantage of our PVC-CM model is the ability to determine whether NA recovers in parallel

FIGURE 5 Proarrhythmia in PVC-CM and Recovery

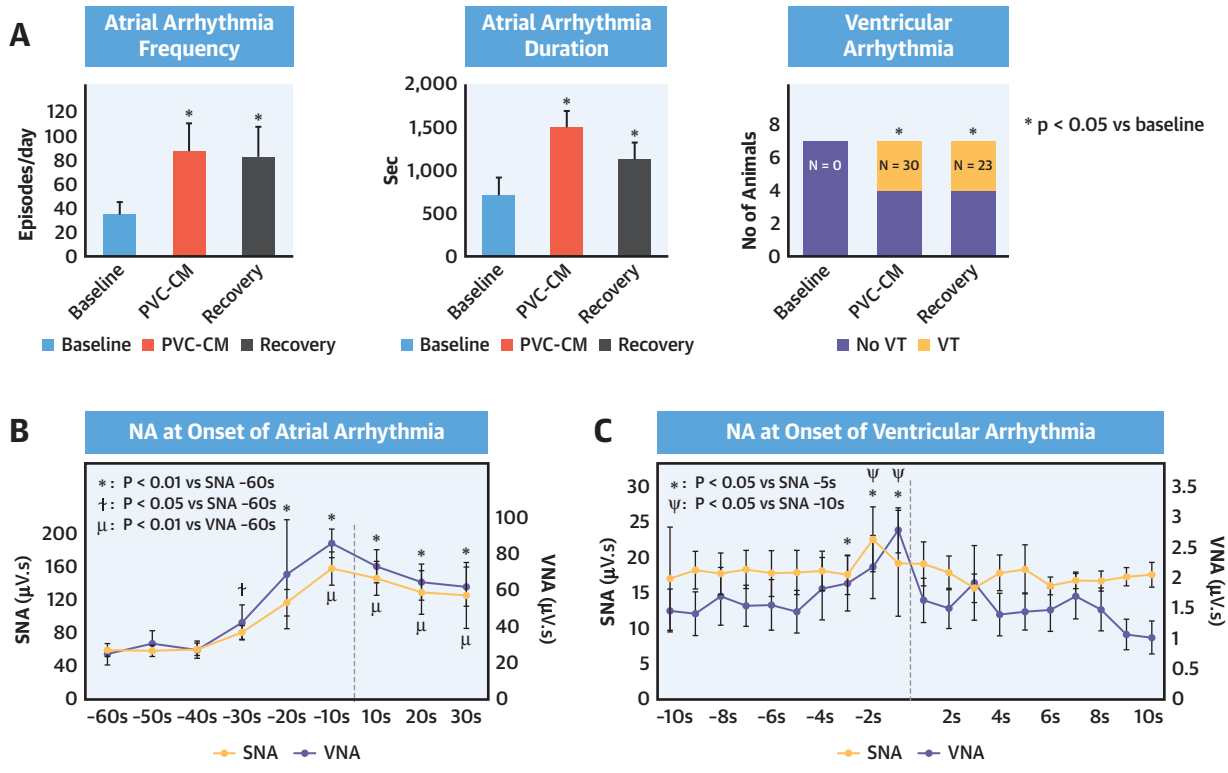

(A) Increased atrial and ventricular arrhythmia burden with PVC-CM and temporal relationship between autonomic nerve activity (NA) and onset of atrial **(B)** and ventricular **(C)** arrhythmia. Abbreviations as in Figure 1.

with LVEF. We note that the increase in SNA tracked reductions in LVEF and dP/dT, and conversely, partial SNA recovery was associated with resolution of LV dysfunction, suggesting that SNA changes are in part a dynamic adaption to the mechanical cardiac dysfunction caused by PVCs. However, the incompleteness of SNA recovery also suggests that the mechanism of sympathetic upregulation in PVC-CM is unique to PVC-CM and not solely related to LV dysfunction per se. Conversely, SNA changes may also contribute to the pathogenesis of PVC-CM, a potentially important therapeutic prospect that merits further exploration.

MECHANISMS OF ACUTE SYMPATHETIC PERTUBATION BY PVCs. PVCs are hypothesized to provoke the CANS via a complex neural reflex pathway involving arterial and cardiac baroreceptors and intrinsic cardiac autonomic nerves that feed back on efferent nerves in the extrinsic CANS to regulate the cardiac response (5,11). Muscle sympathetic nerve recordings in humans demonstrated that burst sympathetic nerve discharge initiates at the diastolic pressure nadir following a PVC beat because of baroreceptor deactivation and terminates with the systolic peak of the post-PVC beat (12) because of baroreceptor activation that inhibits efferent sympathetic outflow. In an in vivo porcine model, Hamon et al. (5) demonstrated that acute PVCs, especially those with variable coupling, cause potent firing of intrinsic cardiac autonomic nerves. Smith et al. (6) found that frequent PVCs trigger increased muscle sympathetic nerve activity and coronary sinus norepinephrine levels. However, the acute and chronic effects of PVCs on sympathovagal nerve activity in normal and PVC-CM hearts remain unknown. In normal hearts (baseline), short-term PVC application triggers an acute increase in SNA but not VNA (Figure 6A). This was accompanied by a gradual increase in BP (Figure 6B) caused by post-extrasystolic potentiation (13), which, in turn, moderated further SNA increases via baroreflex activation (14). However, the SNA response to PVCs was greater in amplitude and duration in PVC-CM compared with normal hearts. This is despite a greater increase in BP (Figure 6B and C), which would have otherwise tempered SNA increase via baroreflex

FIGURE 6 Effect of Acute (1-m) Quadrigeminal PVC Challenge (200 ms coupling) on NA and BP at Baseline, PVC-CM, and Recovery

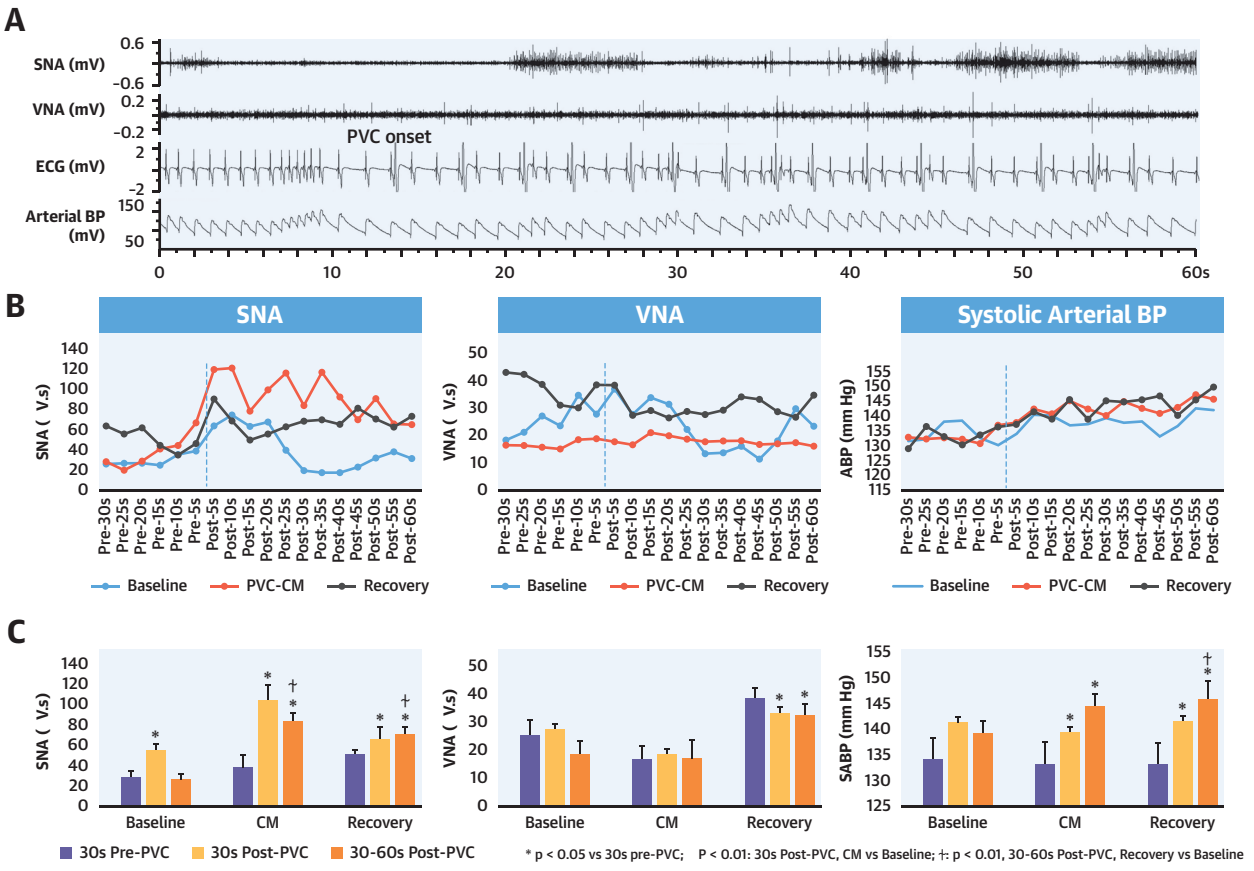

(**A**) Acute SNA increase within seconds after PVC onset, followed by a slower rise in systolic BP. (**B**) Mean systolic BP and integrated NA over 5-s period, before and after onset of PVC. (**C**) Comparison of NA and mean systolic BP in 30-s segments before versus after onset of PVC. Abbreviations as in Figures 1, 4, and 5.

activation (14). Increased SNA response to PVCs persisted in recovered PVC-CM hearts when compared with baseline (normal hearts). These data suggest that baroreflex blunting has occurred in PVC-CM. Because our studies were performed in a nonanesthetized state, the results reflect real-life autonomic physiology conducive to baroreflex assessment. We conclude that PVCs perturb the CANS by a complex interplay of mechanisms that trigger SNA by baroreflex deactivation then suppress SNA by baroreflex activation. This dynamic balance of opposing forces becomes altered in PVC-CM and remains altered despite LV function recovery. We propose that neural remodeling in the CANS (i.e., sympathetic hyperinnervation in the SG) increases the magnitude of SNA response to PVCs, whereas baroreflex blunting results in a more prolonged SNA response to PVCs. Baroreflex blunting carries an adverse prognosis in patients with heart disease (15), underscoring the potential significance of neural remodeling and baroreflex alteration in current or recently recovered PVC-CM.

PROARRHYTHMIA AND NEURAL REMODELING. The presence and arrhythmogenic significance of chronic sympathetic upregulation in PVC-CM remain unknown. In the current study, we report increased burden of both atrial and ventricular arrhythmias in PVC-CM. There was a significant temporal correlation between ventricular arrhythmia onset and SNA increase, and between atrial arrhythmias and acute SNA and VNA increase, suggesting that the arrhythmias are neurally triggered. Clonidine, an inhibitor of central sympathetic output (16), significantly diminished SNA and abolished these arrhythmias after PVC-CM developed. These data indicate that SNA is a critical trigger for both atrial and ventricular arrhythmias in PVC-CM. In addition to an arrhythmic trigger, sympathetic neural remodeling creates a

FIGURE 7 **Sympathetic Neural Remodeling in PVC-CM**

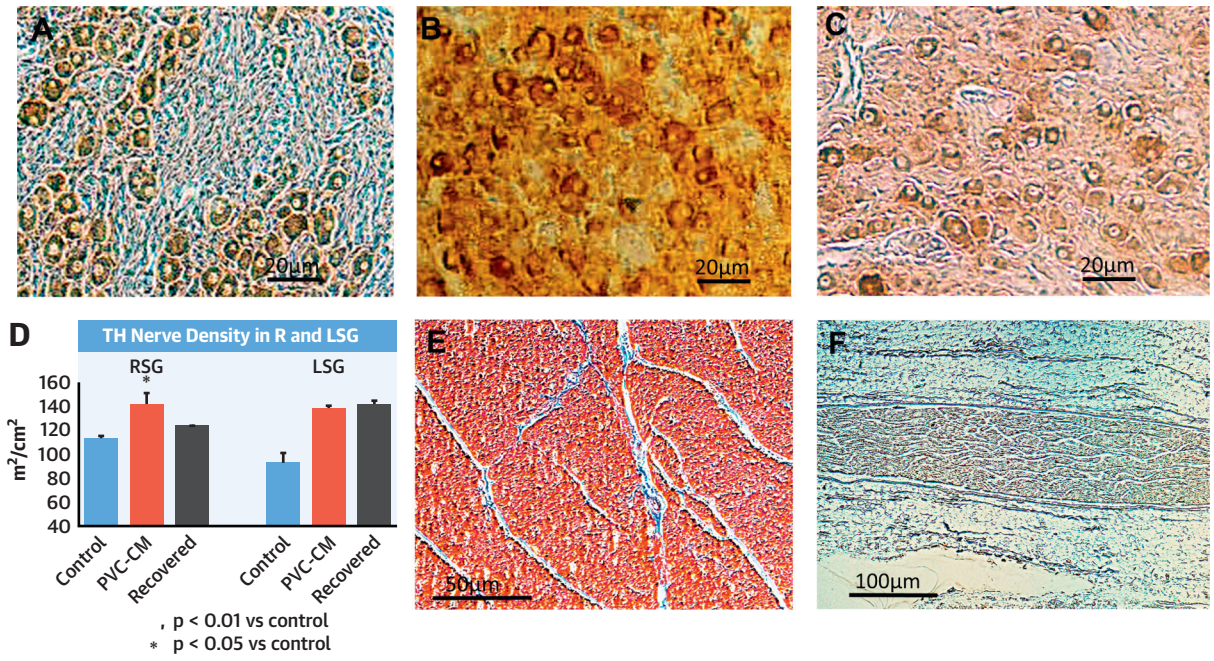

Immunostaining with tyrosine hydroxylase (TH) antibodies of left and right stellate ganglia (LSG, RSG) in sham control (N = 5), PVC-CM (N = 5), and PVC-CM–recovered (N = 7) groups. (**A**) LSG sham control. (**B**) LSG PVC-CM. (**C**) LSG recovered PVC-CM. (**D**) Comparison of TH nerve density in R versus LSG. (**E**) Lack of interstitial fibrosis in PVC-CM. (**F**) Choline acetyltransferase (ChAT) staining of L cardiac vagus nerve. Abbreviations as in Figure 1.

proarrhythmic substrate in PVC-CM. We hypothesize that this substrate derives from critical interactions between elevated sympathetic tone with cellular electrophysiological remodeling in PVC-CM. The latter includes heterogeneous reductions of IK_1, ICa_L and I_{to}, leading to increased dispersion of ventricular action potential duration and refractoriness as we previously reported (17). In electrophysiologically remodeled hearts, PVCs in the presence of sympathetic stimulation induces greater beat-to-beat electrical conduction and repolarization abnormalities than in normal hearts (18). Conversely, we demonstrated that neural remodeling promoted greater PVC burden and greater sympathetic responses to evoked PVCs. Therefore, the combination of neural and electrical remodeling in PVC-CM may lead to a vicious cycle and perfect storm for malignant ventricular arrhythmias.

ROLE OF NEURAL REMODELING IN PATHOGENESIS OF PVC-CM. Although chronic sympathetic upregulation is present in PVC-CM, it remains unclear whether it is a cause or effect of PVC-CM. We previously reported in our canine PVC-CM model decreases in L-type calcium channel current and protein subunit, decreases in calcium-induced calcium release, and dyad scaffolding protein junctophilin (17). On the other hand, sympathetic stimulation increases L-type calcium current by beta-receptor–stimulated cyclic AMP-dependent phosphorylation of L-type calcium channel, thus increasing cardiac inotropy (19). Therefore, sympathetic upregulation may be a compensatory mechanism for abnormal calcium handling and LV systolic dysfunction in PVC-CM. However, sympathetic upregulation itself has been shown to depress myocardial function via the direct toxic effects of norepinephrine on cardiac myocytes with resulting necrosis and apoptosis and impaired beta-adrenoreceptor function (20). Another potential pathophysiologic link between sympathetic upregulation and PVC-CM is via proarrhythmia. Neural remodeling promotes increased PVCs (and other arrhythmias), which, in turn, trigger increased SNA, leading to a vicious cycle of proarrhythmia and arrhythmia-induced CM (PVC-CM vs. tachycardia-induced CM), regardless of the initiating stimulus (3). Further studies are needed to clarify the role of sympathetic neural remodeling in the pathogenesis of PVC-CM.

STELLATE GANGLIA NEURAL REMODELING. Our histology studies indicate that neural remodeling is limited to the SG sparing the cardiac vagal nerve and sympathetic nerves within the ventricular myocardium. This is in contrast to tachypacing models of cardiomyopathy (21) or to human systolic heart failure (22), which are characterized by significant sympathetic hyperinnervation within the heart. The differences in neural, electrophysiological, and structural remodeling between PVC-CM (7,17) and conventional models (21,22) of systolic cardiomyopathy suggest that the mechanisms of remodeling in PVC-CM are unique to PVC-CM. The sparing of ventricular myocardium in PVC-CM could also be due to the less severe extent of LV dysfunction compared with tachypacing models, evidenced by the absence of clinical heart failure and normal pro-BNP levels in our model (8) or to the relatively short duration of exposure to PVCs. On the other hand, the absence of remodeling of the vagus may contribute to sympathetic excess in PVC-CM and after its recovery. Remodeled SG could be a proarrhythmic substrate and thus a potential therapeutic target for PVC-CM, similar to left cardiac sympathetic denervation for ventricular arrhythmia storm (23).

STUDY LIMITATIONS. The intrinsic CANS has been shown to be an important modulator of cardiac response to PVCs (5). We, however, did not record NA from the intrinsic CANS in this study. We also did not measure serum norepinephrine levels. We selected 4 weeks as an appropriate time course for recovery of LVEF, based on previous findings (7). However, a longer study may be necessary to determine if further recovery of SNA occurs. Our animal model was limited by the use of fixed coupled PVCs from the RV apex. Although our data suggest an important pathophysiologic role of neural remodeling in PVC-CM, whether elevated sympathetic tone per se is causative of PVC-CM remains unresolved.

CONCLUSIONS

Neural remodeling in PVC-CM is characterized by extracardiac sympathetic hyperinnervation, resulting in imbalanced sympathetic neural hyperactivity, increased atrial and ventricular proarrhythmia, and exaggerated sympathetic firing in response to PVCs. This sympathovagal imbalance and proarrhythmia persist despite resolution of PVC-CM.

ACKNOWLEDGMENT The authors thank Marcus Thames, MD, for his helpful review of the manuscript.

ADDRESS FOR CORRESPONDENCE: Dr. Alex Y. Tan, Electrophysiology Section, Division of Cardiology, Hunter Holmes McGuire VA Medical Center,1201 Broad Rock Blvd, Richmond, VA 23220. E-mail: alex.tan@va.gov. Twitter: @RichmondVAMC.

PERSPECTIVES

COMPETENCY IN PATIENT CARE AND PROCEDURAL SKILLS: In patients with cardiomyopathy related to chronic premature ventricular contractions (PVC-CM), neural remodeling may result in a persisting proarrhythmic substrate despite suppression of PVC.

TRANSLATIONAL OUTLOOK: Additional research is needed to develop novel therapeutic approaches aimed at preventing neural remodeling or modulating autonomic tone to reduce the risk of ventricular arrhythmias in patients with PVC-CM.

REFERENCES

1. Yarlagadda RK, Iwai S, Stein KM, et al. Reversal of cardiomyopathy in patients with repetitive monomorphic ventricular ectopy originating from the right ventricular outflow tract. Circulation 2005;112:1092–7.

2. Penela D, Van Huls Van Taxis C, Aguinaga L, et al. Neurohormonal, structural, and functional recovery pattern after premature ventricular complex ablation is independent of structural heart disease status in patients with depressed left ventricular ejection fraction: a prospective multicenter study. J Am Coll Cardiol 2013;62:1195–202.

3. Huizar JF, Ellenbogen KA, Tan AY, Kaszala K. Arrhythmia-induced cardiomyopathy. J Am Coll Cardiol 2019;73:2328–44.

4. Noda T, Shimizu W, Taguchi A, et al. Malignant entity of idiopathic ventricular fibrillation and polymorphic ventricular tachycardia initiated by premature extrasystoles originating from the right ventricular outflow tract. J Am Coll Cardiol 2005;46:1288–94.

5. Hamon D, Rajendran PS, Chui RW, et al. Premature ventricular contraction coupling interval variability destabilizes cardiac neuronal and electrophysiological control: insights from simultaneous cardioneural mapping. Circ Arrhythm Electrophysiol 2017;10:e004937.

6. Smith ML, Hamdan MH, Wasmund SL, et al. High-frequency ventricular ectopy can increase sympathetic neural activity in humans. Heart Rhythm 2010;7:497–503.

7. Huizar JF, Kaszala K, Potfay J, et al. Left ventricular systolic dysfunction induced by ventricular ectopy: a novel model for premature ventricular contraction-induced cardiomyopathy. Circ Arrhythm Electrophysiol 2011;4:543–9.

8. Tan AY, Hu YL, Potfay J, et al. Impact of ventricular ectopic burden in a premature ventricular contraction-induced cardiomyopathy animal model. Heart Rhythm 2016;13:755–61.

9. Tan AY, Zhou S, Ogawa M, et al. Neural mechanisms of paroxysmal atrial fibrillation and paroxysmal atrial tachycardia in ambulatory canines. Circulation 2008;118:916–25.

10. Tan AY, Li H, Wachsmann-Hogiu S, Chen LS, Chen P-S, Fishbein MC. Autonomic innervation and segmental muscular disconnections at the human

pulmonary vein-atrial junction: implications for catheter ablation of atrial-pulmonary vein junction. J Am Coll Cardiol 2006;48:132–43.

11. Lombardi F, Ruscone TG, Malliani A. Premature ventricular contractions and reflex sympathetic activation in cats. Cardiovasc Res 1989;23:205–12.

12. Smith ML, Ellenbogen KA, Eckberg DL. Baseline arterial pressure affects sympathoexcitatory responses to ventricular premature beats. Am J Physiol 1995;269:H153–9.

13. Cooper MW. Postextrasystolic potentiation: do we really know what it means and how to use it? Circulation 1993;88:2962–71.

14. Minisi AJ, Dibner-Dunlap M, Thames MD. Vagal cardiopulmonary baroreflex activation during phenylephrine infusion. Am J Physiol 1989;257:R1147–53.

15. La Rovere MT, Bigger JT, Marcus FI, Mortara A, Schwartz PJ. Baroreflex sensitivity and heart-rate variability in prediction of total cardiac mortality after myocardial infarction: ATRAMI (Autonomic Tone and Reflexes After Myocardial Infarction) Investigators. Lancet 1998;351:478–84.

16. Isaac L. Clonidine in the central nervous system: site and mechanism of hypotensive action. J Cardiovasc Pharmacol 1980;1 suppl 2:S5–19.

17. Wang Y, Eltit JM, Kaszala K, et al. Cellular mechanism of premature ventricular contraction-induced cardiomyopathy. Heart Rhythm 2014;11:2064–72.

18. Vaseghi M, Lux RL, Mahajan A, Shivkumar K. Sympathetic stimulation increases dispersion of repolarization in humans with myocardial infarction. Am J Physiol Heart Circ Physiol 2012;302:H1838–46.

19. Hartzell HC, Méry PF, Fischmeister R, Szabo G. Sympathetic regulation of cardiac calcium current is due exclusively to cAMP-dependent phosphorylation. Nature 1991;351:573–6.

20. Floras JS. Sympathetic nervous system activation in human heart failure: clinical implications of an updated model. J Am Coll Cardiol 2009;54:375–85.

21. Ogawa M, Zhou S, Tan AY, et al. Left stellate ganglion and vagal nerve activity and cardiac arrhythmias in ambulatory dogs with pacing-induced congestive heart failure. J Am Coll Cardiol 2007;50:335–43.

22. Cao JM, Fishbein MC, Han JB, et al. Relationship between regional cardiac hyperinnervation and ventricular arrhythmia. Circulation 2000;101:1960–9.

23. Ajijola OA, Wisco JJ, Lambert HW, et al. Extracardiac neural remodeling in humans with cardiomyopathy. Circ Arrhythm Electrophysiol 2012;5:1010–116.

KEY WORDS autonomic nervous system, cardiomyopathy, idiopathic ventricular arrhythmia, nonsustained ventricular tachycardia

APPENDIX For an expanded Methods section and supplemental figure, please see the online version of this paper.